

Article

The H₂S Donor GYY4137 Stimulates Reactive Oxygen Species Generation in BV2 Cells While Suppressing the Secretion of TNF and Nitric Oxide

Milica Lazarević¹, Emanuela Mazzon², Miljana Momčilović¹, Maria Sofia Basile^{1,3}, Giuseppe Colletti³, Maria Cristina Petralia², Placido Bramanti², Ferdinando Nicoletti^{3,*} and Đorđe Miljković¹

¹ Department of Immunology, Institute for Biological Research “Siniša Stanković”, University of Belgrade, Bulevar despota Stefana 142, 11060 Belgrade, Serbia; milica.laza93@gmail.com (M.L.); mommilja@yahoo.com (M.M.); sofiabasile@hotmail.it (M.S.B.); georgije_zw@yahoo.com (Đ.M.)

² IRCCS Centro Neurolesi Bonino Pulejo, Strada Statale 113, C.da Casazza, 98124 Messina, Italy; emanuela.mazzon@ircsme.it (E.M.); m.cristinapetralia@gmail.com (M.C.P.); placido.bramanti@ircsme.it (P.B.)

³ Department of Biomedical and Biotechnological Sciences, University of Catania, Via S. Sofia 89, 95123 Catania, Italy; Giuseppecolletti140@hotmail.com

* Correspondence: ferdinic@unict.it; Tel.: +39-095-478-1270

Received: 1 October 2018; Accepted: 7 November 2018; Published: 14 November 2018



Abstract: GYY4137 is a hydrogen sulfide (H₂S) donor that has been shown to act in an anti-inflammatory manner in vitro and in vivo. Microglial cells are among the major players in immunoinflammatory, degenerative, and neoplastic disorders of the central nervous system, including multiple sclerosis, Parkinson’s disease, Alzheimer’s disease, and glioblastoma multiforme. So far, the effects of GYY4137 on microglial cells have not been thoroughly investigated. In this study, BV2 microglial cells were stimulated with interferon-gamma and lipopolysaccharide and treated with GYY4137. The agent did not influence the viability of BV2 cells in concentrations up to 200 μM. It inhibited tumor necrosis factor but not interleukin-6 production. Expression of CD40 and CD86 were reduced under the influence of the donor. The phagocytic ability of BV2 cells and nitric oxide production were also affected by the agent. Surprisingly, GYY4137 upregulated generation of reactive oxygen species (ROS) by BV2 cells. The effect was mimicked by another H₂S donor, Na₂S, and it was not reproduced in macrophages. Our results demonstrate that GYY4137 downregulates inflammatory properties of BV2 cells but increases their ability to generate ROS. Further investigation of this unexpected phenomenon is warranted.

Keywords: hydrogen sulfide; GYY4137; microglia; reactive oxygen species; inflammation

1. Introduction

Hydrogen sulfide (H₂S) is a gaseous signaling molecule that has anti-inflammatory and cytoprotective properties [1]. H₂S is endogenously synthesized from l-cysteine in reactions catalyzed by cystathionine beta-synthase (CBS, EC 4.2.1.22) and gamma-cystathionase (CSE, EC 4.4.1.1) [2].

It has been suggested that H₂S exerts neuroprotective effects in neuroinflammatory diseases, including neurodegenerative diseases, such as Parkinson’s disease, Alzheimer’s disease, and stroke, and autoimmune diseases of the central nervous system (CNS), such as multiple sclerosis [3–5].

More recently, a role for H₂S has also been hypothesized in glioblastoma multiforme (GBM) and neuroblastoma in light of the finding that the expression and activity of CBS, gamma-cystathionase (CTH, EC 4.4.1.1), and 3-mercaptopyruvate sulfurtransferase (MPST, EC 2.8.1.2) were found in the

human glioblastoma-astrocytoma (U-87 MG) and neuroblastoma (SHSY5Y) cell lines [6]. In both cell lines, the expression and activity of MPST was the highest among the investigated enzymes, suggesting its possible role in the generation of H₂S. The higher expression and activity of CBS, CTH, and MPST in the neuroblastoma cells were associated with more intensive generation of H₂S in the presence of 2 mM of cysteine. A threefold higher level of sulfane sulfur, a potential source of H₂S, was detected in the astrocytoma cells in comparison to the neuroblastoma cells [6].

Accordingly, it has been proposed that H₂S donors might be used as therapeutics for brain diseases [7]. Various H₂S donors have been used in biomedical studies investigating the role of H₂S in homeostasis and various pathologies [8]. While NaHS has been predominantly used in the studies, GYY4137 is a slow-releasing H₂S donor that has been increasingly employed over the past 10 years. GYY4137 is a water-soluble derivative of Lawesson's reagent that releases H₂S via hydrolysis [8].

Microglia play a central role in the pathogenesis of various brain diseases, including neurodegenerative and autoimmune disorders and brain cancers [9,10]. In the steady state microglial cells largely contribute to the homeostasis of the CNS [11]. However, under excessive pro-inflammatory activation, they become highly pro-inflammatory and can contribute to autoimmune, degenerative, and neoplastic disorders of the CNS [9]. Activated microglia release various inflammatory and neurotoxic molecules that destroy the CNS tissue and contribute to various neurological disorders [9,10]. Microglial cells are able to perform phagocytosis and to present antigens to T cells through expression of major histocompatibility complex (MHC) molecules and costimulatory molecules, such as cluster of differentiation (CD)80 and CD40 [10]. Through release of inflammatory cytokines, such as tumor necrosis factor (TNF), interleukin (IL)-6 and IL-1 β , and of nitric oxide (NO) and reactive oxygen species (ROS), they contribute to the pathology of various brain diseases, such as Parkinson's disease, Alzheimer's disease, or multiple sclerosis [9,10]. Regarding the role of glial cells in CNS oncogenesis, we and others have shown that dysregulated production of pro-inflammatory cytokines such as macrophage migration inhibitory factor (MIF) from glial cells and in the tumor microenvironment may contribute to the development, maintenance, and aggressiveness of GBM [12–14]. Therefore, regulation of microglia function may represent an important therapeutic target for the treatment of these disorders [9,11].

Along this line of research, we studied here the effects of GYY4137 on BV2 microglial cells. Reduction of TNF and NO release and downregulation of expression of antigen-presenting molecules, but upregulation of ROS generation, was observed under the influence of GYY4137. The obtained results are discussed in relation to the potential use of H₂S donors as therapeutics for CNS diseases.

2. Results

2.1. GYY4137 Inhibits Production of NO and TNF in BV2 Cells

BV2 cells were stimulated with interferon- γ (IFN- γ) and lipopolysaccharide (LPS) and exposed to various concentrations of GYY4137. There was no effect on BV2 cell viability after 24 h of cultivation even with the highest concentration applied (200 μ M), as deduced by crystal violet (CV) and 3-(4,5-dimethylthiazol-2-yl)-2,5-diphenyltetrazolium bromide (MTT) tests (Figure 1A). The result was corroborated with annexin V staining, as there was no change in the percentage of apoptotic BV2 cells after the treatment with 200 μ M of GYY4137 (Figure 1B). At the same time, levels of nitrites, as the measure of NO production, were reduced in the supernatants of GYY4137-treated cultures (Figure 1C). Similarly, TNF but not IL-6 levels in the supernatants were also reduced under the influence of GYY4137 (Figure 1D,E). Interestingly, the effects on TNF production were not paralleled with the inhibition of its RNA expression (Figure 1F).

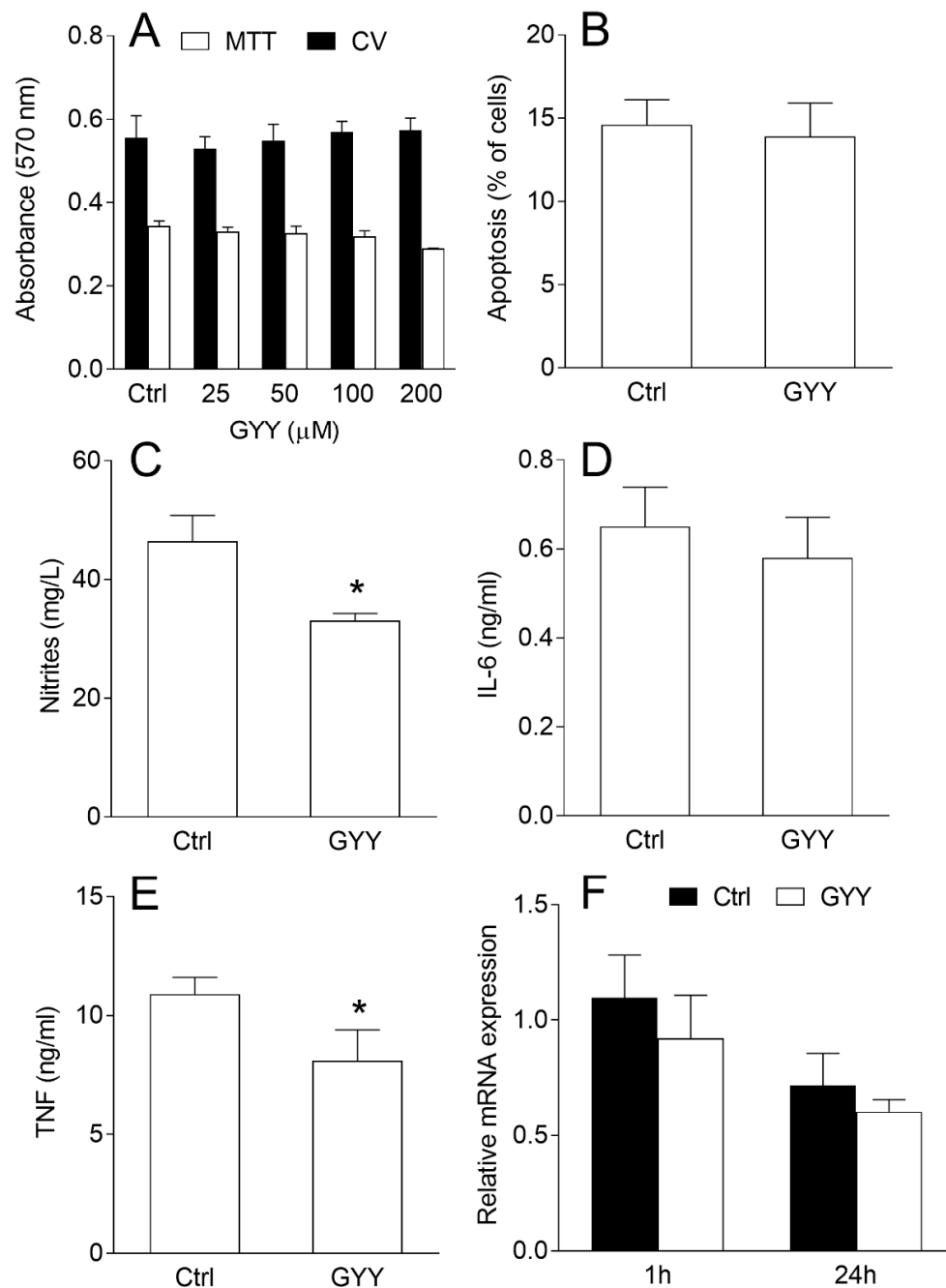


Figure 1. Effects of GYY4137 (GYY) on viability and nitric oxide (NO) and cytokine production in BV2 cells. BV2 cells were stimulated with interferon- γ (IFN- γ) and lipopolysaccharide (LPS) and cultivated in the presence of dimethyl sulfoxide (DMSO) (control—Ctrl) as the vehicle or GYY (200 μ M in **B–F**) for 24 h. Subsequently, the cell viability was determined by crystal violet (CV) and 3-(4,5-dimethylthiazol-2-yl)-2,5-diphenyltetrazolium bromide (MTT) tests (**A**), apoptosis was detected by annexin V staining and cytofluorimetry (**B**), nitrites were measured by Griess reaction (**C**), cytokine concentrations were determined by ELISA (**D,E**), and mRNA expression relative to β -actin by real-time RT-PCR (**F**). Data are presented as mean + standard deviation (SD) from at least three independent experiments. * $p < 0.05$ refers to Ctrl.

2.2. GYY4137 Influences BV2 Cell Phenotype and Phagocytic Ability

In order to determine the effects of GYY4137 on the antigen-presenting function of BV2 cells, expression of costimulatory molecules CD86 and CD40 and phagocytosis of latex beads were

determined. GYY4137 decreased expression of both molecules on BV2 cells (Figure 2A–D). It also inhibited phagocytosis of the latex beads by BV2 cells (Figure 2E,F).

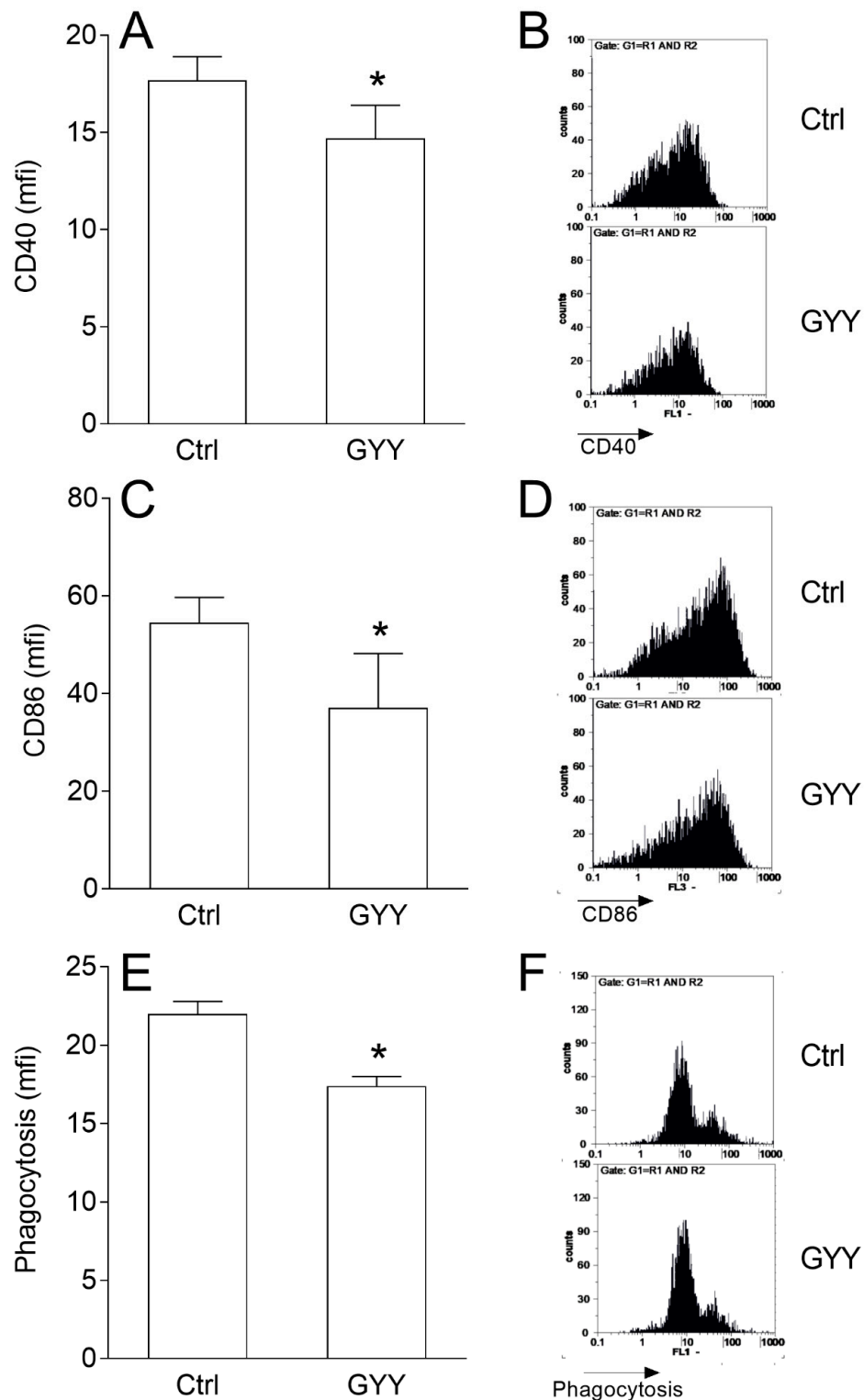


Figure 2. Effects of GYY4137 (GYY) on phenotype and phagocytosis in BV2 cells. BV2 cells were stimulated with IFN- γ and LPS and cultivated in the presence of DMSO (Ctrl) as the vehicle or GYY (200 μ M) for 24 h. Subsequently, expression of CD40 (A,B), CD86 (C,D), and phagocytosis (E,F) were determined by cytofluorimetry. Data are presented as mean + SD from at least three independent experiments (A,C,E). Representative plots are also provided (B,D,F). * $p < 0.05$ refers to Ctrl.

2.3. GYY4137 Upregulates ROS Generation in BV2 Cells

BV2 cells were incubated with GYY4137 for different time periods, ranging from 10 min to 24 h, in the presence or absence of IFN- γ and LPS, and then they were stained with dihydrorhodamine 123 (DHR) and treated with phorbol 12-myristate 13-acetate (PMA) or IFN- γ and LPS to stimulate ROS generation. GYY4137 increased ROS production, as indicated by DHR fluorescence intensity, in BV2 cells in all cases (Figure 3A–D), even after only 10 min of incubation. The ability of GYY4137 to act quickly upon BV2 cells was confirmed by real-time cell analysis, where it was shown that GYY4137 acted in the very first minutes of its application, and that it also had a prolonged effect on BV2 cells (Figure 3E). To exclude the possibility that GYY4137 interacted with DHR regardless of BV2 cells, DHR and GYY4137 were co-incubated in a cell free system and fluorescence was detected by a fluorometer. No GYY4137-imposed increase in fluorescence was observed in the cell-free system (Figure 3F). The effects of GYY4137 were mimicked by another H₂S donor, Na₂S (Figure 3G), thus supporting the idea that increase of ROS in BV2 cells under the influence of GYY4137 was H₂S dependent. This was further corroborated with the fact that GYY4137 that was incubated at 37 °C for 4 days before being used for the treatment of BV2 cells (“spent GYY”) partially lost its ROS-inducing activity (Figure 3H). In order to further test the results obtained with DHR, BV2 cells were stained with the other ROS detector, 2',7'-Dichlorofluorescein diacetate (DCFDA), and an increase of ROS generation under the influence of GYY4137 was detected once again (Figure 3I). Finally, the effects of GYY4137 on ROS generation in macrophages were explored. No increase in ROS production in macrophages under the influence of GYY4137 was observed (Figure 3J,K), hence suggesting microglia-specific ROS-increasing effects of GYY4137.

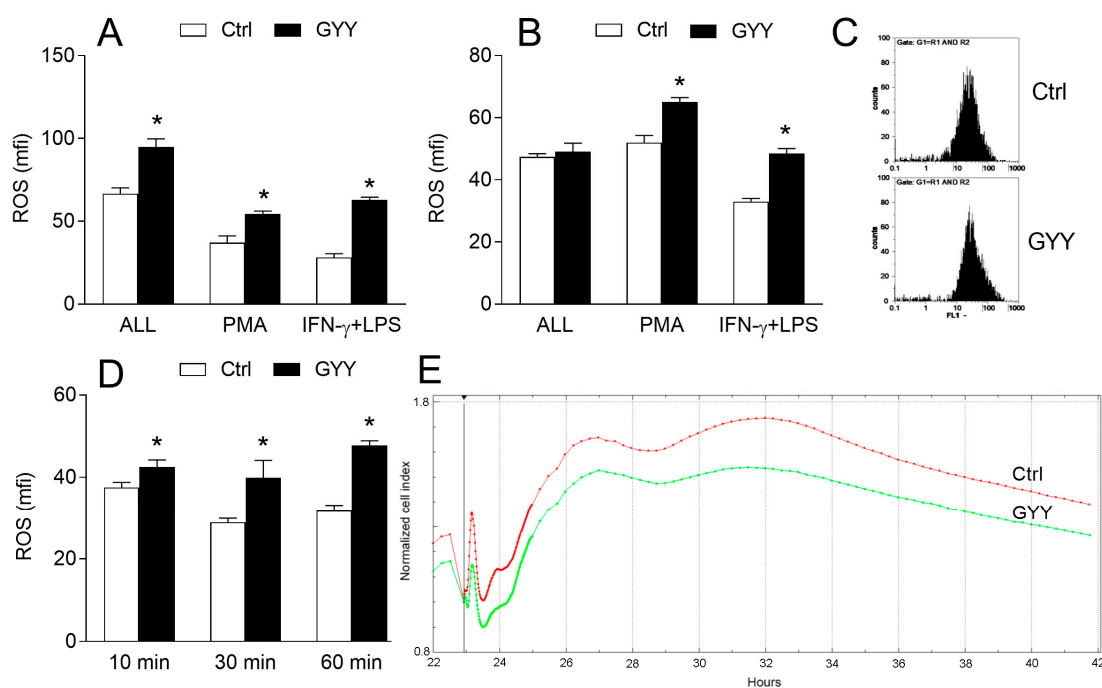


Figure 3. Cont.

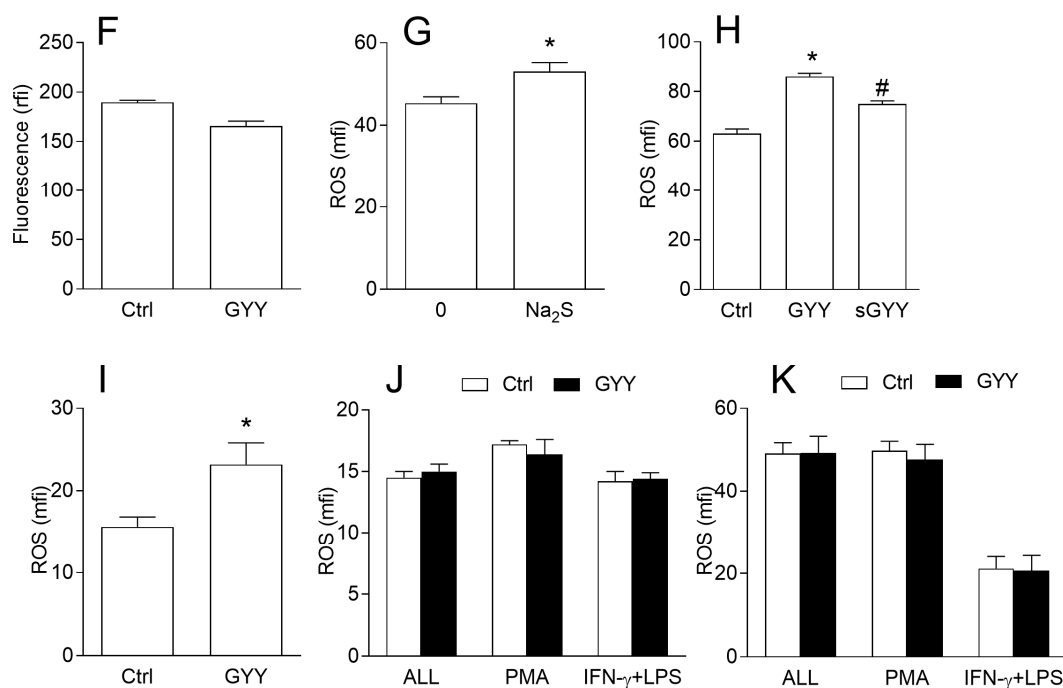


Figure 3. Effects of GYY4137 (GYY) on reactive oxygen species (ROS) production in BV2 cells. BV2 cells were cultivated in the presence of DMSO (Ctrl) as the vehicle or GYY (200 μ M). (A) BV2 cells were treated with IFN- γ and LPS and DMSO or GYY for 24 h, stained with DHR, and stimulated with phorbol 12-myristate 13-acetate (PMA) for 90 min (ALL), or they were treated with DMSO or GYY for 24 h, stained with DHR, and stimulated with PMA or IFN- γ and LPS (IFN- γ + LPS) for 90 min. Subsequently, cytofluorimetry was performed. (B) Same as A, except that incubation lasted for 1 h instead of 24 h. (C) Representative DHR plots from (B). (D) BV2 cells were treated with DMSO or GYY for the indicated time periods, stained with DHR, stimulated with PMA, and cytofluorimetry was performed. (E) BV2 cells were treated with IFN- γ and LPS and DMSO or GYY and analyzed by the real-time cell analyzer. Representative plot is provided. (F) DMSO or GYY were mixed with DHR in a cell-free system and fluorescence was detected on a fluorimeter. (G) BV2 cells were treated with Na₂S (200 μ M) or were untreated (0) for 60 min, stained with DHR, and stimulated with PMA for 90 min. Subsequently, cytofluorimetry was performed. (H) BV2 cells were treated with DMSO or GYY for 60 min, stained with DCFDA, and stimulated with PMA for 90 min. Subsequently, cytofluorimetry was performed. (I) Same as B (PMA), with additional treatment with “spent” GYY4137 (sGYY). (J) Same as B (PMA), except that BV2 cells were stained with DCFDA (K). Same as B, except that mouse macrophages were used. (K) Same as B, except that rat macrophages were used. Data are presented as mean + SD from at least three independent experiments. * $p < 0.05$ refers to Ctrl or 0; # $p < 0.05$ refers to difference between GYY and sGYY.

3. Discussion

We have shown here that the H₂S donor GYY4137 exerted pleiotropic effects on BV2 cells in vitro that included inhibitory effects on NO and TNF generation and expression of CD40 and CD86 along with clear-cut stimulation of ROS production.

The eventual significance of these effects of GYY4137 on BV2 cells in neurological pathologies, if any, must be proved in adequate in vivo studies. The inhibitory effects of GYY4137 on NO and TNF production may be beneficial in neuroimmunological diseases such as multiple sclerosis and neurodegenerative disorders, as these molecules are implicated as important mediators in their pathogenesis [15,16]. Also, downregulation of costimulatory molecules CD86 and CD40, which are important for efficient antigen presentation by microglial cells and are elevated in these cells during autoimmune events in the CNS [17], could be beneficial in CNS-directed autoimmune responses. The effects of H₂S donors on BV2 cells have been previously studied [18]. In agreement with our data,

GY4137 inhibited LPS-induced NO generation both in BV2 cells and in the macrophage cell line RAW264.7 [18,19]. Differences in the effects of H₂S on cytokine production in different monocytic cell lines have also been reported. In contrast to the report on RAW264.7 cells [19], it was shown that NaHS stimulated TNF, IL-6, and IL-1 β in U937 monocytic cell lines [20]. The different experimental conditions used may also account for the divergent effects of GYY4137 on the TNF secretory capacity of RAW264.7 cells and U937 cells [19,20]. However, these data indicate that the effects of H₂S donors on immune cells are divergent, and that in various settings, H₂S activates or inhibits immune cells [2].

The observation of ROS potentiation in BV2 cells under the influence of GYY4137 was unexpected, as it was shown that H₂S inhibits ROS generation in neuronal cells and protected cardiac cells against ROS effects [21–24]. Therefore, the ROS-potentiating effect of GYY4137 in BV2 cells was explored in numerous additional control experiments described in Section 2.3 that convergently support the finding that GYY4137 stimulates BV2 cells to generate ROS through H₂S release. Although this phenomenon is unusual, it has been described previously in independent studies. It was shown that H₂S-imposed hepatotoxicity is mediated through ROS induction [25]. H₂S genotoxic effects on Chinese hamster ovary cells were also mediated through ROS [26]. Furthermore, H₂S induced oxidative DNA and RNA damage in coelomocytes of marine invertebrates [27]. Interestingly, positive effects of H₂S on ROS generation were also reported in plants, where H₂S-stimulated H₂O₂ production in *Arabidopsis* guard cells was implicated in stomatal closure [28]. Finally, it was reported that H₂S inhibited growth of *Escherichia coli* through induction of ROS [29]. Thus, ROS-mediated effects of H₂S have been observed in evolutionarily distant organisms. The significance of upregulated production of ROS induced by H₂S may warrant further investigations.

There are numerous reports on the beneficial effects of H₂S in various brain pathologies. H₂S protects neurons from cell death provoked by oxidative glutamate toxicity or anoxia/reoxygenation [30,31]. The neuroprotective effects of H₂S donors were also observed in vivo [32–35]. Furthermore, NaHS or GYY4137 counteracted inflammation as well as oxidative and nitrosative stress in animal models of Alzheimer's disease [36], Parkinson's disease [37], high-salt-induced hypertension [38], and cerebral malaria [39]. Importantly, the protective effects of H₂S in hypoxia-induced neurotoxicity in vivo were shown to be mediated through inhibition of microglial activation, including NO and cytokine generation [40]. Similarly, anti-inflammatory effects of NaHS in a repetitive febrile seizure model were paralleled with inhibition of microglial activity [41]. Moreover, endogenous H₂S was shown to be of great importance for microglial shift from pro- to anti-inflammatory in cerebral ischemia [42].

Our results are in concordance with these data as far as NO and TNF are concerned. As discussed, the major discordant result is the observed potentiation of ROS by GYY4137 in BV2 cells. However, negative effects of H₂S on brain pathology, such as cerebral ischemic damage, were also previously reported [43]. As it was postulated that cerebral ischemic damage is mediated through ROS [44,45], it would be important to examine if the damage-potentiating effects of H₂S are ROS dependent. Also, caution should be exercised when considering ROS strictly as pro-inflammatory and damaging mediators. It is well known that both ROS and H₂S are not only effector but also signaling molecules working through thiol-based and other redox switches [46]. H₂S-mediated ROS generation might have regulatory rather than effector properties and it is, therefore, essential to test the observed effects of GYY4137 on microglial cells in various settings in which microglial cells interact with other cells.

On the other hand, the presently observed combined downregulation of NO and TNF along with the upregulation of ROS allows us to hypothesize that H₂S donors may be useful for the treatment of + certain brain tumors such as GBM. In fact, it is known that the local production of pro-inflammatory cytokines such as MIF and TNF [47–49] in the tumor microenvironment of solid tumors such as GBM and melanoma induce the production of NO and other immunosuppressive mediators that may favor growth and invasiveness of GBM [12,13]. Vice versa, experimental chemotherapeutic drugs exert their action on the viability of GBM cell lines through local production of ROS and subsequent JNK activation [50,51].

Like the other endogenous gas NO, which has been indicated both as an oncogenic and oncosuppressor molecule, with its ultimate fate probably depending on concentration and time of exposure [52], conflicting data have been generated on the chemotherapeutic potential of H₂S donors or H₂S inducers. This observed pharmacological profile of GYY4137 in BV2 cells warrants additional *in vivo* studies of H₂S and its donors and inducers also in the field of neuro-oncology [53,54].

Defining the eventual suitable area of application of H₂S in CNS disorders would be of immediate utility for the clinical setting, as several H₂S-releasing drugs, such as SG1002 for cardiovascular disorders and ATB-346 for arthritis, have progressed into clinical trials and could be tested in CNS pathologies of neuroinflammatory, neurodegenerative, or neoplastic origin once clear-cut proof of concepts have been generated in relevant animal models [55].

4. Materials and Methods

4.1. Cell Cultures and Reagents

Unless specifically stated, chemicals used in the experiments were from Sigma-Aldrich (St. Louis, MO, USA). BV2 cells were obtained as the kind gift of Dr. Alba Minelli, Università degli Studi di Perugia, Perugia, Italy. BV2 cells were grown and cultured in RPMI-1640 culture medium (Biological Industries, Kibbutz Beit-Haemek, Israel) that was supplemented with 5% heat-inactivated fetal calf serum (FCS, PAA Laboratories, Pasching, Austria) at 37 °C in a humidified atmosphere containing 5% CO₂. For the treatments, BV2 cells were seeded at 5×10^5 /mL/well in 24-well plates (Sarstedt, Pasching, Austria). BV2 cells were stimulated with 10 ng/mL of recombinant mouse IFN- γ and 100 ng/mL of LPS and treated with various concentrations of GYY4137 (Cayman Chemical, Ann Arbor, MI, USA).

4.2. Viability Assays

Viability of BV2 was assessed by CV and MTT tests. At the end of the treatment, cells were washed with phosphate-buffered saline (PBS) to remove nonadherent dead cells. For the CV test, the remaining cells were fixed with methanol. After staining with 1% CV solution, the plates were thoroughly washed and then the dye was dissolved in 33% acetic acid. For the MTT assay, adherent BV2 cell were exposed to 0.5 μ g/mL MTT solution and incubated for 30 min at 37 °C. Cell culture supernatants were removed and dimethyl sulfoxide (DMSO) was added to the plates to dissolve the formazan crystals. The absorbance of dissolved dyes, corresponding to the number of viable cells, was measured in triplicates at 540 nm with a correction at 670 nm using an automated microplate reader (LKB 5060-006, LKB, Vienna, Austria).

4.3. Detection of NO Release

Nitrite accumulation, a measure of NO release, was determined in cell culture supernatants using the Griess reaction. In brief, triplicate aliquots of cell-free supernatants were mixed with an equal volume of Griess reagent (1:1 mixture of 0.1% naphthylethylenediamine dihydrochloride and 1% sulphanilamide in 5% H₃PO₄). The absorbance at 540 nm was determined with a microplate reader and compared to a standard curve for NaNO₂.

4.4. ELISA Test for Determination of Cytokines

Cytokine concentration in cell culture supernatants was determined by sandwich ELISA using MaxiSorp plates (Nunc, Roskilde, Denmark) and anticytokine paired antibodies according to the manufacturer's instructions. Samples were analyzed in duplicates for murine TNF (eBioscience, San Diego, CA, USA) and murine IL-6 (Abcam, Cambridge, UK). The results were calculated using standard curves made on the basis of known concentrations of the appropriate recombinant cytokines.

4.5. Real-Time Reverse Transcription Polymerase Chain Reaction

Total RNA was isolated from cells using a mi-Total RNA Isolation Kit (Metabion, Martinsried, Germany) and reverse transcribed using random hexamer primers and MMLV (Moloney Murine Leukemia Virus) reverse transcriptase according to the manufacturer's instructions (Fermentas, Vilnius, Lithuania). Prepared cDNAs were amplified by using Maxima SYBR Green/ROX qPCR Master Mix (Fermentas, Vilnius, Lithuania) according to the recommendations of the manufacturer in an ABI PRISM 7000 Sequence Detection System (Applied Biosystems, Foster City, CA, USA). Thermocycler conditions comprised an initial step at 50 °C for 5 min, followed by a step at 95 °C for 10 min, and a subsequent two-step PCR program at 95 °C for 15 s and 60 °C for 60 s for 40 cycles. The PCR primers (Metabion, Martinsried, Germany) were as follows: TNF: 5'-CCA CGT AGC AAA CCA C-3'; 5'-TGG GTG AGG AGC ACG TAG T-3'; (GenBank accession no. NM 013693.2) and β -actin: 5'-CCA GCG CAG CGA TAT CG-3'; 5'-GCT TCT TTG CAG CTC CTT CGT-3'; (GenBank acc. No. NM_007393.3). Accumulation of PCR products was detected in real time and the results were analyzed with 7500 System Software (Applied Biosystems, Foster City, CA, USA). Relative RNA expression is presented as 2^{-dCt} , where dCt is the difference between Ct values of a gene of interest and the endogenous control (β -actin).

4.6. Cytofluorimetry

BV2 cells were stained with FITC-conjugated anti-CD40 (eBioscience, San Diego, CA, USA) and Pe-Cy5-conjugated anti-CD86 (eBioscience, San Diego, CA, USA). Appropriate isotype control antibodies were used where necessary to set gates for cell marker positivity. Typically, proportion of isotype control antibody-stained cells was <1%. Detection of apoptosis was performed via annexin V-FITC staining (Biotium, Hayward, CA, USA). Cells positive for annexin V-FITC were considered apoptotic. For detection of phagocytosis, BV2 cells were plated in 24-well plates at 1×10^5 /well and pretreated with GYY4137 for 24 h. Latex beads (1 μ m, yellow-green) were preopsonized in PBS supplemented with 50% FCS. Medium was discarded and the preopsonized beads were added (10 beads per cell), and cells were incubated at 37 °C for an additional hour. BV2 cells were analyzed with a CyFlow Space flow cytometer (Partec, Munster, Germany). Results of cytofluorimetry are presented as the proportion of cells bound by an appropriate antibody or as mean fluorescent intensity (mfi) of cell population. Cells were gated on live cells (R1) according to FSC vs. SSC and on cell singlets (R2) according to FSC vs. FSC-width, and mfi (arithmetic mean) was determined for all the cells within G1 (R1 and R2) by FloMax software for cytometry (Partec, Munster, Germany).

4.7. Detection of Reactive Oxygen Species (ROS) Generation

For detection of ROS generation, DHR or DCFDA staining was performed. The cells were incubated in the presence of 5 μ M of DHR or 5 μ M of DCFDA for 20 min. BV2 cells were pre-incubated with GYY4137 in the presence of IFN- γ (10 ng/mL) and LPS (100 ng/mL) for the indicated time periods, stained with DHR, and then stimulated with PMA (100 ng/mL) for an additional 90 min. Alternatively, BV2 cells were pre-incubated with GYY4137 for the indicated time periods, stained with DHR or DCFDA, and then stimulated with PMA (100 ng/mL) or IFN- γ (10 ng/mL) and LPS (100 ng/mL). The fluorescence was acquired via flow cytometry.

4.8. Real-Time Cell Analysis

Cell activation was characterized in real time by using an xCELLigence RTCA DP analyzer (Roche Diagnostics, Pleasanton, CA, USA). BV2 cells were seeded at 2.5×10^4 cells into each well of an E-Plate 16 (Roche Diagnostics, Pleasanton, CA, USA). After 24 h of initial adherence, BV2 cells were treated with IFN- γ (10 ng/mL) and LPS (100 ng/mL) and GYY4137 (200 μ M) or DMSO (solvent control). Impedance measurements were recorded every 15 s during the first 2 h of cultivation and

then every 15 min overnight. Impedance measurements were recorded as a combined cellular index of proliferation, viability, activation, and morphology changes.

4.9. Statistical Analysis

Data were analyzed using two-way ANOVA followed by Tukey's test or by Student's *t*-test, as appropriate. A *p*-value less than 0.05 was considered statistically significant.

Author Contributions: M.L. performed the main experimental work; M.M. supervised the experimental work, analyzed and critically revised the data; F.N. conceived and designed the study and critically revised the manuscript; D.M. conceived and designed the study, supervised the work, analyzed and interpreted the data, drafted the work, and critically revised the manuscript; E.M. and P.B. critically revised the manuscript and provided funds; M.S.B., M.C.P., and G.C. critically revised and edited the manuscript. All authors made significant contributions in this study and approved the final version to be published.

Funding: This study was supported by current research funds 2018 of IRCCS "Centro Neurolesi Bonino Pulejo", Messina-Italy and by the Ministry of Education, Science and Technological Development of the Republic of Serbia (173035 and 173013).

Conflicts of Interest: The authors declare no conflict of interest.

References

- Wallace, J.L.; Blackler, R.W.; Chan, M.V.; Da Silva, G.J.; Elsheikh, W.; Flannigan, K.L.; Gamaniek, I.; Manko, A.; Wang, L.; Motta, J.-P.; et al. Anti-inflammatory and cytoprotective actions of hydrogen sulfide: translation to therapeutics. *Antioxid. Redox Signal.* **2015**, *22*, 398–410. [[CrossRef](#)] [[PubMed](#)]
- Fagone, P.; Mazzon, E.; Bramanti, P.; Bendtzen, K.; Nicoletti, F. Gasotransmitters and the immune system: Mode of action and novel therapeutic targets. *Eur. J. Pharmacol.* **2018**, *834*, 92–102. [[CrossRef](#)] [[PubMed](#)]
- Gong, Q.-H.; Shi, X.-R.; Hong, Z.-Y.; Pan, L.-L.; Liu, X.-H.; Zhu, Y.-Z. A new hope for neurodegeneration: possible role of hydrogen sulfide. *J. Alzheimers Dis.* **2011**, *24* (Suppl. 2), 173–182. [[CrossRef](#)]
- Xue, X.; Bian, J.-S. Neuroprotective effects of hydrogen sulfide in Parkinson's disease animal models: methods and protocols. *Methods Enzymol.* **2015**, *554*, 169–186. [[PubMed](#)]
- Talaei, F. Pathophysiological Concepts in Multiple Sclerosis and the Therapeutic Effects of Hydrogen Sulfide. *Basic Clin. Neurosci.* **2016**, *7*, 121–136. [[CrossRef](#)] [[PubMed](#)]
- Bronowicka-Adamska, P.; Bentke, A.; Wróbel, M. Hydrogen sulfide generation from l-cysteine in the human glioblastoma-astrocytoma U-87 MG and neuroblastoma SHSY5Y cell lines. *Acta Biochim. Pol.* **2017**, *64*, 171–176. [[CrossRef](#)] [[PubMed](#)]
- Zhang, J.; Ding, Y.; Wang, Z.; Kong, Y.; Gao, R.; Chen, G. Hydrogen sulfide therapy in brain diseases: from bench to bedside. *Med. Gas Res.* **2017**, *7*, 113. [[PubMed](#)]
- Powell, C.R.; Dillon, K.M.; Matson, J.B. A review of hydrogen sulfide (H₂S) donors: Chemistry and potential therapeutic applications. *Biochem. Pharmacol.* **2018**, *149*, 110–123. [[CrossRef](#)] [[PubMed](#)]
- Du, L.; Zhang, Y.; Chen, Y.; Zhu, J.; Yang, Y.; Zhang, H.-L. Role of Microglia in Neurological Disorders and Their Potentials as a Therapeutic Target. *Mol. Neurobiol.* **2017**, *54*, 7567–7584. [[CrossRef](#)] [[PubMed](#)]
- O'Loughlin, E.; Madore, C.; Lassmann, H.; Butovsky, O. Microglial Phenotypes and Functions in Multiple Sclerosis. *Cold Spring Harb. Perspect. Med.* **2018**, *8*, a028993. [[CrossRef](#)] [[PubMed](#)]
- Colonna, M.; Butovsky, O. Microglia Function in the Central Nervous System During Health and Neurodegeneration. *Annu. Rev. Immunol.* **2017**, *35*, 441–468. [[CrossRef](#)] [[PubMed](#)]
- Mangano, K.; Mazzon, E.; Basile, M.S.; Di Marco, R.; Bramanti, P.; Mammana, S.; Petralia, M.C.; Fagone, P.; Nicoletti, F. Pathogenic role for macrophage migration inhibitory factor in glioblastoma and its targeting with specific inhibitors as novel tailored therapeutic approach. *Oncotarget* **2018**, *9*, 17951–17970. [[CrossRef](#)] [[PubMed](#)]
- Presti, M.; Mazzon, E.; Basile, M.S.; Petralia, M.C.; Bramanti, A.; Colletti, G.; Bramanti, P.; Nicoletti, F.; Fagone, P. Overexpression of macrophage migration inhibitory factor and functionally-related genes, D-DT, CD74, CD44, CXCR2 and CXCR4, in glioblastoma. *Oncol. Lett.* **2018**, *16*, 2881–2886. [[CrossRef](#)] [[PubMed](#)]
- Yeung, Y.; McDonald, K.; Grewal, T.; Munoz, L. Interleukins in glioblastoma pathophysiology: implications for therapy. *Br. J. Pharmacol.* **2013**, *168*, 591–606. [[CrossRef](#)] [[PubMed](#)]

15. Sugama, S.; Takenouchi, T.; Cho, B.P.; Joh, T.H.; Hashimoto, M.; Kitani, H. Possible roles of microglial cells for neurotoxicity in clinical neurodegenerative diseases and experimental animal models. *Inflamm. Allergy Drug Targets* **2009**, *8*, 277–284. [[CrossRef](#)] [[PubMed](#)]
16. Zindler, E.; Zipp, F. Neuronal injury in chronic CNS inflammation. *Best Pract. Res. Clin. Anaesthesiol.* **2010**, *24*, 551–562. [[CrossRef](#)] [[PubMed](#)]
17. Ponomarev, E.D.; Shriver, L.P.; Maresz, K.; Dittel, B.N. Microglial cell activation and proliferation precedes the onset of CNS autoimmunity. *J. Neurosci. Res.* **2005**, *81*, 374–389. [[CrossRef](#)] [[PubMed](#)]
18. Zhou, X.; Cao, Y.; Ao, G.; Hu, L.; Liu, H.; Wu, J.; Wang, X.; Jin, M.; Zheng, S.; Zhen, X.; et al. CaMKK β -Dependent Activation of AMP-Activated Protein Kinase Is Critical to Suppressive Effects of Hydrogen Sulfide on Neuroinflammation. *Antioxid. Redox Signal.* **2014**, *21*, 1741–1758. [[CrossRef](#)] [[PubMed](#)]
19. Whiteman, M.; Li, L.; Rose, P.; Tan, C.-H.; Parkinson, D.B.; Moore, P.K. The effect of hydrogen sulfide donors on lipopolysaccharide-induced formation of inflammatory mediators in macrophages. *Antioxid. Redox Signal.* **2010**, *12*, 1147–1154. [[CrossRef](#)] [[PubMed](#)]
20. Zhi, L.; Ang, A.D.; Zhang, H.; Moore, P.K.; Bhatia, M. Hydrogen sulfide induces the synthesis of proinflammatory cytokines in human monocyte cell line U937 via the ERK-NF-kappaB pathway. *J. Leukoc. Biol.* **2007**, *81*, 1322–1332. [[CrossRef](#)] [[PubMed](#)]
21. Lan, A.; Liao, X.; Mo, L.; Yang, C.; Yang, Z.; Wang, X.; Hu, F.; Chen, P.; Feng, J.; Zheng, D.; et al. Hydrogen sulfide protects against chemical hypoxia-induced injury by inhibiting ROS-activated ERK1/2 and p38MAPK signaling pathways in PC12 cells. *PLoS ONE* **2011**, *6*, e25921. [[CrossRef](#)] [[PubMed](#)]
22. Dong, X.-B.; Yang, C.-T.; Zheng, D.-D.; Mo, L.-Q.; Wang, X.-Y.; Lan, A.-P.; Hu, F.; Chen, P.-X.; Feng, J.-Q.; Zhang, M.-F.; et al. Inhibition of ROS-activated ERK1/2 pathway contributes to the protection of H₂S against chemical hypoxia-induced injury in H9c2 cells. *Mol. Cell. Biochem.* **2012**, *362*, 149–157. [[CrossRef](#)] [[PubMed](#)]
23. Luo, Y.; Yang, X.; Zhao, S.; Wei, C.; Yin, Y.; Liu, T.; Jiang, S.; Xie, J.; Wan, X.; Mao, M.; et al. Hydrogen sulfide prevents OGD/R-induced apoptosis via improving mitochondrial dysfunction and suppressing an ROS-mediated caspase-3 pathway in cortical neurons. *Neurochem. Int.* **2013**, *63*, 826–831. [[CrossRef](#)] [[PubMed](#)]
24. Kumar, M.; Sandhir, R. Neuroprotective Effect of Hydrogen Sulfide in Hyperhomocysteinemia Is Mediated Through Antioxidant Action Involving Nrf2. *Neuromol. Med.* **2018**. [[CrossRef](#)] [[PubMed](#)]
25. Eghbal, M.A.; Pennefather, P.S.; O'Brien, P.J. H₂S cytotoxicity mechanism involves reactive oxygen species formation and mitochondrial depolarisation. *Toxicology* **2004**, *203*, 69–76. [[CrossRef](#)] [[PubMed](#)]
26. Attene-Ramos, M.S.; Wagner, E.D.; Gaskins, H.R.; Plewa, M.J. Hydrogen Sulfide Induces Direct Radical-Associated DNA Damage. *Mol. Cancer Res.* **2007**, *5*, 455–459. [[CrossRef](#)] [[PubMed](#)]
27. Joyner-Matos, J.; Predmore, B.L.; Stein, J.R.; Leeuwenburgh, C.; Julian, D. Hydrogen Sulfide Induces Oxidative Damage to RNA and DNA in a Sulfide-Tolerant Marine Invertebrate. *Physiol. Biochem. Zool.* **2010**, *83*, 356–365. [[CrossRef](#)] [[PubMed](#)]
28. Scuffi, D.; Nietzel, T.; Di Fino, L.M.; Meyer, A.J.; Lamattina, L.; Schwarzländer, M.; Laxalt, A.M.; García-Mata, C. Hydrogen Sulfide Increases Production of NADPH Oxidase-Dependent Hydrogen Peroxide and Phospholipase D-Derived Phosphatidic Acid in Guard Cell Signaling. *Plant Physiol.* **2018**, *176*, 2532–2542. [[CrossRef](#)] [[PubMed](#)]
29. Fu, L.-H.; Wei, Z.-Z.; Hu, K.-D.; Hu, L.-Y.; Li, Y.-H.; Chen, X.-Y.; Han, Z.; Yao, G.-F.; Zhang, H. Hydrogen sulfide inhibits the growth of *Escherichia coli* through oxidative damage. *J. Microbiol.* **2018**, *56*, 238–245. [[CrossRef](#)] [[PubMed](#)]
30. Kimura, Y.; Kimura, H. Hydrogen sulfide protects neurons from oxidative stress. *FASEB J.* **2004**, *18*, 1165–1167. [[CrossRef](#)] [[PubMed](#)]
31. Shao, J.-L.; Wan, X.-H.; Chen, Y.; Bi, C.; Chen, H.-M.; Zhong, Y.; Heng, X.-H.; Qian, J.-Q. H₂S Protects Hippocampal Neurons from Anoxia–Reoxygenation Through cAMP-Mediated PI3K/Akt/p70S6K Cell-Survival Signaling Pathways. *J. Mol. Neurosci.* **2011**, *43*, 453–460. [[CrossRef](#)] [[PubMed](#)]
32. Chu, Q.-J.; He, L.; Zhang, W.; Liu, C.-L.; Ai, Y.-Q.; Zhang, Q. Hydrogen sulfide attenuates surgical trauma-induced inflammatory response and cognitive deficits in mice. *J. Surg. Res.* **2013**, *183*, 330–336. [[CrossRef](#)] [[PubMed](#)]
33. Jiang, X.; Huang, Y.; Lin, W.; Gao, D.; Fei, Z. Protective effects of hydrogen sulfide in a rat model of traumatic brain injury via activation of mitochondrial adenosine triphosphate-sensitive potassium channels and reduction of oxidative stress. *J. Surg. Res.* **2013**, *184*, e27–e35. [[CrossRef](#)] [[PubMed](#)]

34. Zhang, Q.; Yuan, L.; Liu, D.; Wang, J.; Wang, S.; Zhang, Q.; Gong, Y.; Liu, H.; Hao, A.; Wang, Z. Hydrogen sulfide attenuates hypoxia-induced neurotoxicity through inhibiting microglial activation. *Pharmacol. Res.* **2014**, *84*, 32–44. [[CrossRef](#)] [[PubMed](#)]
35. Yu, Q.; Lu, Z.; Tao, L.; Yang, L.; Guo, Y.; Yang, Y.; Sun, X.; Ding, Q. ROS-Dependent Neuroprotective Effects of NaHS in Ischemia Brain Injury Involves the PARP/AIF Pathway. *Cell. Physiol. Biochem.* **2015**, *36*, 1539–1551. [[CrossRef](#)] [[PubMed](#)]
36. Giuliani, D.; Ottani, A.; Zaffe, D.; Galantucci, M.; Strinati, F.; Lodi, R.; Guarini, S. Hydrogen sulfide slows down progression of experimental Alzheimer's disease by targeting multiple pathophysiological mechanisms. *Neurobiol. Learn. Mem.* **2013**, *104*, 82–91. [[CrossRef](#)] [[PubMed](#)]
37. Hou, X.; Yuan, Y.; Sheng, Y.; Yuan, B.; Wang, Y.; Zheng, J.; Liu, C.-F.; Zhang, X.; Hu, L.-F. GYY4137, an H₂S Slow-Releasing Donor, Prevents Nitritative Stress and α -Synuclein Nitration in an MPTP Mouse Model of Parkinson's Disease. *Front. Pharmacol.* **2017**, *8*, 741. [[CrossRef](#)] [[PubMed](#)]
38. Liang, Y.-F.; Zhang, D.-D.; Yu, X.-J.; Gao, H.-L.; Liu, K.-L.; Qi, J.; Li, H.-B.; Yi, Q.-Y.; Chen, W.-S.; Cui, W.; et al. Hydrogen sulfide in paraventricular nucleus attenuates blood pressure by regulating oxidative stress and inflammatory cytokines in high salt-induced hypertension. *Toxicol. Lett.* **2017**, *270*, 62–71. [[CrossRef](#)] [[PubMed](#)]
39. Jiang, P.; Xu, Z.; Xiao, B.; Han, Z.; Huang, J.; Xu, J.; Lun, Z.; Zhou, W. Hydrogen sulfide protects against the development of experimental cerebral malaria in a C57BL/6 mouse model. *Mol. Med. Rep.* **2017**, *16*, 2045–2050. [[CrossRef](#)] [[PubMed](#)]
40. Zhang, M.; Shan, H.; Chang, P.; Wang, T.; Dong, W.; Chen, X.; Tao, L. Hydrogen Sulfide Offers Neuroprotection on Traumatic Brain Injury in Parallel with Reduced Apoptosis and Autophagy in Mice. *PLoS ONE* **2014**, *9*, e87241. [[CrossRef](#)] [[PubMed](#)]
41. Zhuang, F.; Zhou, X.; Li, H.; Yang, X.; Dong, Z.; Zhou, W.; Chen, J. Hydrogen Sulfide Promotes Learning and Memory and Suppresses Proinflammatory Cytokines in Repetitive Febrile Seizures. *Neuroimmunomodulation* **2016**, *23*, 271–277. [[CrossRef](#)] [[PubMed](#)]
42. Zhang, M.; Wu, X.; Xu, Y.; He, M.; Yang, J.; Li, J.; Li, Y.; Ao, G.; Cheng, J.; Jia, J. The cystathionine β -synthase/hydrogen sulfide pathway contributes to microglia-mediated neuroinflammation following cerebral ischemia. *Brain. Behav. Immun.* **2017**, *66*, 332–346. [[CrossRef](#)] [[PubMed](#)]
43. Qu, K.; Chen, C.P.L.H.; Halliwell, B.; Moore, P.K.; Wong, P.T.-H. Hydrogen Sulfide Is a Mediator of Cerebral Ischemic Damage. *Stroke* **2006**, *37*, 889–893. [[CrossRef](#)] [[PubMed](#)]
44. Juurlink, B.H.; Sweeney, M.I. Mechanisms that result in damage during and following cerebral ischemia. *Neurosci. Biobehav. Rev.* **1997**, *21*, 121–128. [[CrossRef](#)]
45. Wong, P.T.H.; Qu, K.; Chimon, G.N.; Seah, A.B.H.; Chang, H.M.; Wong, M.C.; Ng, Y.K.; Rumpel, H.; Halliwell, B.; Chen, C.P.L.H. High Plasma Cyst(e)ine Level May Indicate Poor Clinical Outcome in Patients With Acute Stroke: Possible Involvement of Hydrogen Sulfide. *J. Neuropathol. Exp. Neurol.* **2006**, *65*, 109–115. [[CrossRef](#)] [[PubMed](#)]
46. Longen, S.; Beck, K.-F.; Pfeilschifter, J. H₂S-induced thiol-based redox switches: Biochemistry and functional relevance for inflammatory diseases. *Pharmacol. Res.* **2016**, *111*, 642–651. [[CrossRef](#)] [[PubMed](#)]
47. Nicoletti, F.; Créange, A.; Orlikowski, D.; Bolgert, F.; Mangano, K.; Metz, C.; Di Marco, R.; Al Abed, Y. Macrophage migration inhibitory factor (MIF) seems crucially involved in Guillain-Barré syndrome and experimental allergic neuritis. *J. Neuroimmunol.* **2005**, *168*, 168–174. [[CrossRef](#)] [[PubMed](#)]
48. Fagone, P.; Mazzon, E.; Cavalli, E.; Bramanti, A.; Petralia, M.C.; Mangano, K.; Al-Abed, Y.; Bramati, P.; Nicoletti, F. Contribution of the macrophage migration inhibitory factor superfamily of cytokines in the pathogenesis of preclinical and human multiple sclerosis: In silico and in vivo evidences. *J. Neuroimmunol.* **2018**, *322*, 46–56. [[CrossRef](#)] [[PubMed](#)]
49. Zaccone, P.; Fehérvári, Z.; Blanchard, L.; Nicoletti, F.; Edwards, C.K., III; Cooke, A. Autoimmune thyroid disease induced by thyroglobulin and lipopolysaccharide is inhibited by soluble TNF receptor type I. *Eur. J. Immunol.* **2002**, *32*, 1021–1028. [[CrossRef](#)]
50. Peng, F.; Wang, X.; Shu, M.; Yang, M.; Wang, L.; Ouyang, Z.; Shen, C.; Hou, X.; Zhao, B.; Wang, X.; et al. Raddeanin a Suppresses Glioblastoma Growth by Inducing ROS Generation and Subsequent JNK Activation to Promote Cell Apoptosis. *Cell. Physiol. Biochem.* **2018**, *47*, 1108–1121. [[CrossRef](#)] [[PubMed](#)]

51. Gratton, R.; Tricarico, P.M.; Guimaraes, R.L.; Celsi, F.; Crovella, S. Lopinavir/Ritonavir Treatment Induces Oxidative Stress and Caspaseindependent Apoptosis in Human Glioblastoma U-87 MG Cell Line. *Curr. HIV Res.* **2018**, *16*, 106–112. [[CrossRef](#)] [[PubMed](#)]
52. Maksimovic-Ivanic, D.; Fagone, P.; McCubrey, J.; Bendtzen, K.; Mijatovic, S.; Nicoletti, F. HIV-protease inhibitors for the treatment of cancer: Repositioning HIV protease inhibitors while developing more potent NO-hybridized derivatives? *Int. J. Cancer* **2017**, *140*, 1713–1726. [[CrossRef](#)] [[PubMed](#)]
53. Yang, C.-T.; Chen, L.; Xu, S.; Day, J.J.; Li, X.; Xian, M. Recent Development of Hydrogen Sulfide Releasing/Stimulating Reagents and Their Potential Applications in Cancer and Glycometabolic Disorders. *Front. Pharmacol.* **2017**, *8*, 664. [[CrossRef](#)] [[PubMed](#)]
54. Gemici, B.; Elsheikh, W.; Feitosa, K.B.; Costa, S.K.P.; Muscara, M.N.; Wallace, J.L. H₂S-releasing drugs: Anti-inflammatory, cytoprotective and chemopreventative potential. *Nitric Oxide* **2015**, *46*, 25–31. [[CrossRef](#)] [[PubMed](#)]
55. Wallace, J.L.; Vaughan, D.; Dickey, M.; MacNaughton, W.K.; de Nucci, G. Hydrogen Sulfide-Releasing Therapeutics: Translation to the Clinic. *Antioxid. Redox Signal.* **2018**, *28*, 1533–1540. [[CrossRef](#)] [[PubMed](#)]

Sample Availability: Samples of the compounds are not available from the authors.



© 2018 by the authors. Licensee MDPI, Basel, Switzerland. This article is an open access article distributed under the terms and conditions of the Creative Commons Attribution (CC BY) license (<http://creativecommons.org/licenses/by/4.0/>).